Int. J. Multiphase Flow Vol. 17, No. 4, pp. 455–468, 1991
Printed in Great Britain.

0301-9322/91 $3.00 + 0.00

DROPLET ENTRAINMENT AND DEPOSITION IN HORIZONTAL ANNULAR FLOW

S. V. PARAS and A. J. KARABELAS

Department of Chemical Engineering, University of Thessaloniki and Chemical Process Engineering Research Institute, P.O. Box 1517, 540 06 Thessaloniki, Greece

(Received 15 August 1990; in revised form 20 February 1991)

Abstract—Local measurements of droplet fluxes, in the core of horizontal annular flow, are employed in order to calculate the liquid concentration distribution as well as the circumferential variation of deposition rate. A relatively simple model is proposed for predicting the above quantities. Terms representing fluxes due to turbulent diffusion and gravitational settling are used in the model. An additional parameter **a** is introduced and is considered to represent a combination of fluxes; i.e. the net upward flux of droplets responding to turbulence and the flux of droplets that gain high inertia upon atomization. An interpretation is given of *average* deposition (or atomization) rates obtained from the data, by using detailed information on film thickness properties and by recognizing that only films with a local thickness greater than a critical value can contribute to atomization. The development of a physically realistic correlation for the mean deposition rate is explored.

Key Words: gas–liquid flow, annular flow, droplet distribution, deposition rates

1. INTRODUCTION

The rates of liquid atomization (R_A) and deposition (R_D) are very important parameters in the study of annular gas–liquid flow. In the case of horizontal flow, gravity imposes an asymmetric liquid distribution both in the film at the wall and in the entrained droplets. Thus, the circumferential distributions of atomization and deposition rates are expected to be generally non-uniform. This non-uniformity causes serious difficulties in experimental as well as in modeling efforts. It is not, therefore, surprising that data on local deposition and atomization rates are very meager and that no reliable models are available yet. The very limited data on local deposition reported by Anderson & Russell (1970) in a 2.54 cm pipe and the difficulties encountered in recent modeling attempts by Laurinat *et al.* (1985), Lin *et al.* (1985) and Fukano & Ousaka (1989) confirm the above assessment. On the contrary, in the case of (axisymmetric) *vertical* annular flow there is a considerable amount of information available on droplet concentration distribution as well as on R_D and R_A (e.g. Hutchinson & Whalley 1973; Leman 1985; Schadel 1988; Schadel & Hanratty 1989).

The work reported here is part of an ongoing research effort aimed at improving our understanding and modeling horizontal annular flow. Detailed data are presented on local droplet fluxes in the pipe cross section. For horizontal pipes, a thesis by Williams (1986), reporting on data taken in a 9.53 cm i.d. pipe loop, appears to be the only other study where such detailed measurements are available.

The data sets collected during the course of this work have been utilized in several ways. Using appropriate interpolation and integration techniques, the mean liquid entrainment fraction, $E = W_{LE}/W_L$, has been computed. By transforming the local liquid fluxes to local concentrations, comparisons have been made with a proposed model. Finally, by using measured (or extrapolated) values of droplet concentration close to the pipe wall, the circumferential distribution as well as the mean value of R_D has been obtained.

The above data on local fluxes are complemented with detailed measurements of film thickness properties, analyzed and reported in the companion paper by Paras & Karabelas (1991, this issue, pp. 439–454), as well as with pressure drop measurements. This information is necessary for calculating various flow parameters, as will be outlined in the following sections.

2. DROPLET ENTRAINMENT IN THE GAS

2.1. Flow loop

The experiments are carried out in a recently constructed horizontal flow loop (Paras & Karabelas 1991). Two-phase flow develops in a 16 m long straight section, of 50.8 mm i.d. The mixing section for the two phases is a simple tee with the liquid phase introduced in the branch and the gas phase in the run. The test section is positioned about 300 dia downstream of the mixing section of the two phases and the flow is considered to be fully developed at this location.

2.2. Experimental techniques

One of the most reliable experimental methods to obtain the fraction of liquid dispersed in the gas core is to measure the droplet flux distribution in the pipe cross section and to integrate it. Measurements are made for horizontal annular flow, under various gas and liquid flow rates. An L-shaped sampling tube is inserted into the pipe to collect droplets entrained in the gas core [figure 1(a)]. The tube has a 3.17 mm i.d. and a 0.22 mm wall thickness at the end facing the flow, and extends 10 cm upstream to minimize any local disturbances caused by the vertical tube section entering the pipe. A traversing mechanism is employed to move the pitot tube along the inside diameter of the pipe, whereas the circumferential orientation of the probe is adjusted by rotating the entire test section. With this arrangement it is possible to sample droplets within approx. 3 mm of the pipe wall.

The sampling setup is shown in figure 1(b). Entrained water can be collected in either one of two identical Plexiglas separators, connected in parallel. The flow entering the pitot tube is switched from one of the separators to the other by simultaneously activating two electrically operated three-way valves [E, in figure 1(b)]. One of the separators serves as an auxiliary vessel before and after sampling in order to adjust and maintain constant flow. An air stream is used at the end of each run to totally empty both vessels. To obtain roughly isokinetic conditions, suction is applied to the top of the separators and the air flow from the sampling tube is measured with a rotameter. However, it is observed that exactly isokinetic conditions are not necessary, as is also pointed out by Romano *et al.* (1978).

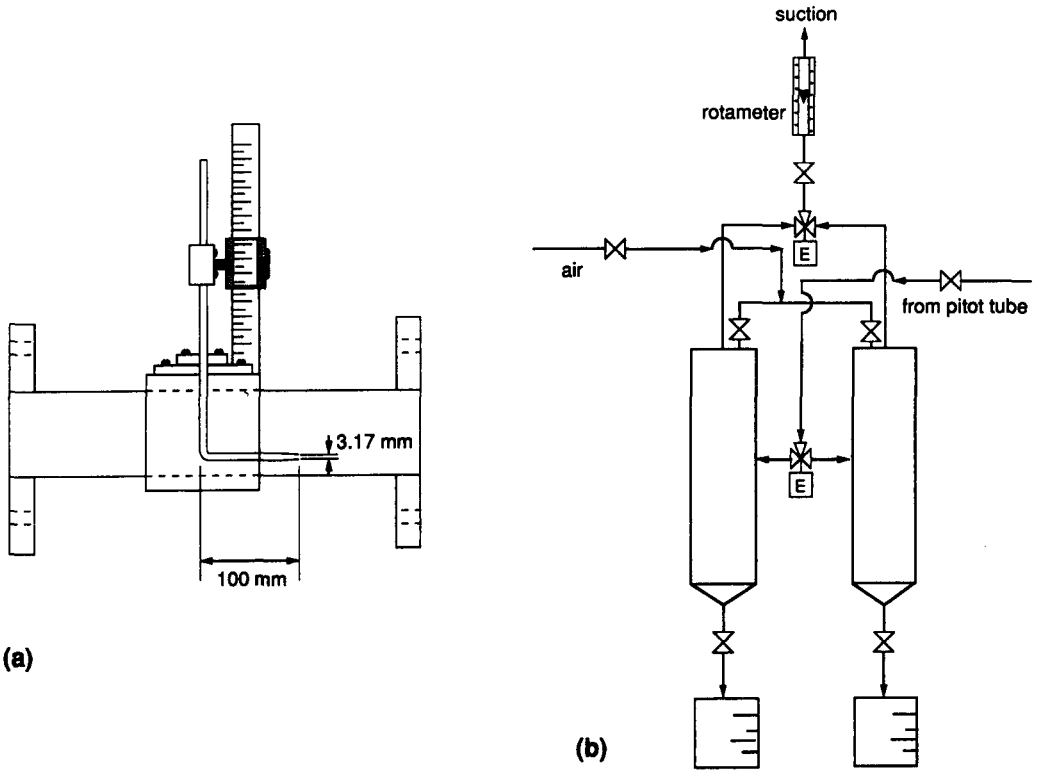

Figure 1. (a) Side view of the test section with a pitot tube; (b) arrangement of sampling vessels.

Table 1. Summary of experimental conditions and results

Run	U_L (m/s)	U_G (m/s)	ρ_G (kg/m^3)	E	f^a ($\times 10^4$)	$\langle C \rangle$ (kg/m^3)	$\hat{C}$ (kg/m^3)	w (m/s)	U^* (m/s)	d_p (μm)	A	k_D (m/s)	$\overline{R_D}$ (kg/m^{2}s)
A	0.03	31.1	1.27	0.15	117	0.153	0.133	0.69	2.37	119	0.53	0.377	0.063
B	0.03	38.1	1.52	0.32	101	0.270	0.215	0.48	2.71	96	0.58	0.426	0.107
C	0.03	49.4	1.67	0.50	90	0.326	0.281	0.31	3.31	72	0.48	0.538	0.175
D	0.06	31.6	1.39	0.14	126	0.269	0.238	0.67	2.51	118	0.63	0.361	0.105
E	0.06	43.0	1.66	0.45	111	0.629	0.533	0.42	3.20	88	0.63	0.443	0.276
F	0.06	48.0	1.78	0.62	106	0.781	0.672	0.36	3.50	80	0.67	0.468	0.365
G	0.09	32.5	1.58	0.21	154	0.595	0.505	0.66	2.85	119	0.72	0.337	0.204
H	0.09	46.5	1.91	0.62	119	1.247	1.205	0.41	3.59	89	0.68	0.409	0.574
I	0.12	30.1	1.55	0.16	174	0.675	0.595	0.76	2.80	131	0.66	0.310	0.234
J	0.12	45.4	2.00	0.75	129	2.083	1.718	0.49	3.64	101	0.67	0.351	0.713
K	0.02	65.5	1.98	0.37	68	0.106	0.091	0.15	3.82	51	—	0.706	0.075
L	0.02	49.6	1.63	0.31	76	0.117	0.101	0.29	3.06	69	0.20	0.568	0.067
M	0.02	32.2	1.40	0.10	81	0.059	0.052	0.63	2.05	113	0.42	0.376	0.024
N	0.03	65.5	2.19	0.58	72	0.282	0.242	0.17	3.94	53	0.26	0.646	0.179
O	0.20	46.8	2.31	0.71	136	3.037	2.670	0.55	3.87	111	0.86	0.297	0.912
P	0.20	31.7	1.65	0.23	177	1.429	1.234	0.77	2.99	133	0.77	0.294	0.453
Q	0.06	61.5	2.33	0.67	82	0.662	0.600	0.22	3.94	61	0.58	0.539	0.368

[a]Obtained from $\Delta P/\Delta L$ measurement.

Droplet fluxes are measured by collecting the liquid in a separator, for a specified time period. The quantity of the collected water ranges from 20 to 80 cm^3. The total amount of liquid entrained in the gas is calculated by using the horizontal and vertical droplet flux profiles and by integrating throughout the pipe cross section. Detailed measurements of film thickness at the pipe wall (Paras & Karabelas 1991) are employed to exclude areas in the pipe cross section occupied by the liquid film. Moreover, the statistical characteristics of the liquid film thickness (mainly the RMS values) are necessary in order to compute an equivalent wall roughness and to estimate the gas velocity distribution.

2.3. Data on droplet fluxes and entrainment

The ranges of superficial velocities, covered in the tests, were $U_L = 2$ to 20 cm/s for water and $U_G = 31$ to 66 m/s for air. Seventeen data sets were collected, as shown in table 1. Three droplet flux profiles were measured for each set of flow rates, i.e. a vertical, a horizontal and one at 45°. Measured vertical and horizontal droplet flux profiles are shown in figures 2 and 3. The strong influence of gravity is evident in the vertical profiles, which exhibit, in general, a smooth variation from pipe top to bottom. However, some vertical flux profiles at high liquid rates (e.g. $U_L = 12$ cm/s in figure 2) display a pronounced local maximum above the pipe centerline. It is not known at present whether this is due to high local droplet velocities, prevailing above the centerline, or to an increase in the local droplet concentration.

The horizontal profiles display a uniform distribution across the pipe diameter, with the exception of a few profiles at high liquid rates. Some relatively minor non-uniformities are within the error bounds of the experimental technique. The uniformity of the flux distribution in the horizontal direction allows a significant simplification in the following modeling effort. Additionally, it is noted that the above general trends in our data are also observed in the data obtained by Williams (1986).

The liquid entrainment fraction, E, is defined as

$$E = \frac{W_{LE}}{W_L} = \frac{W_L - W_{LF}}{W_L},$$

where W_L is the total liquid flow rate, W_{LE} is the entrained liquid flow rate and W_{LF} is the flow rate of the liquid film. The entrainment data from this study are compared with a correlation developed by Williams (1986) and are in very good agreement, as shown in figure 4. This expression correlates satisfactorily data for *air–water* and pipe diameters in the range $D = 25$ to 100 mm. Thus, it may be useful for practical applications, after testing with fluids of various properties.

Another result of possible practical significance is presented in figure 5, where the *average* flux of liquid entrained in the core, $\bar{Q}$, is plotted against *local* flux Q. The latter represents either the flux at the centerline ($r/R = 0.0$) or the arithmetic mean of three local values of Q, at $r/R = -0.6$,

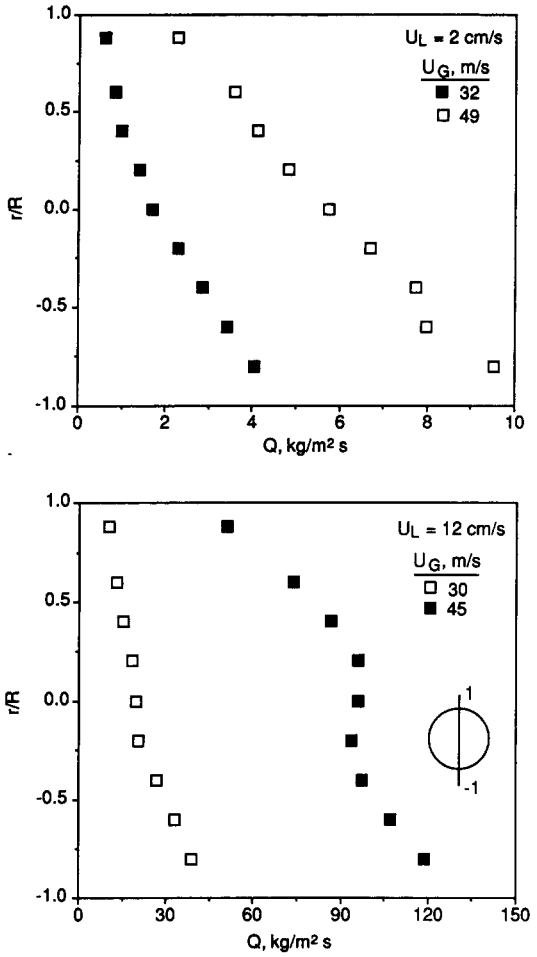

Figure 2. Characteristic vertical droplet flux profiles.

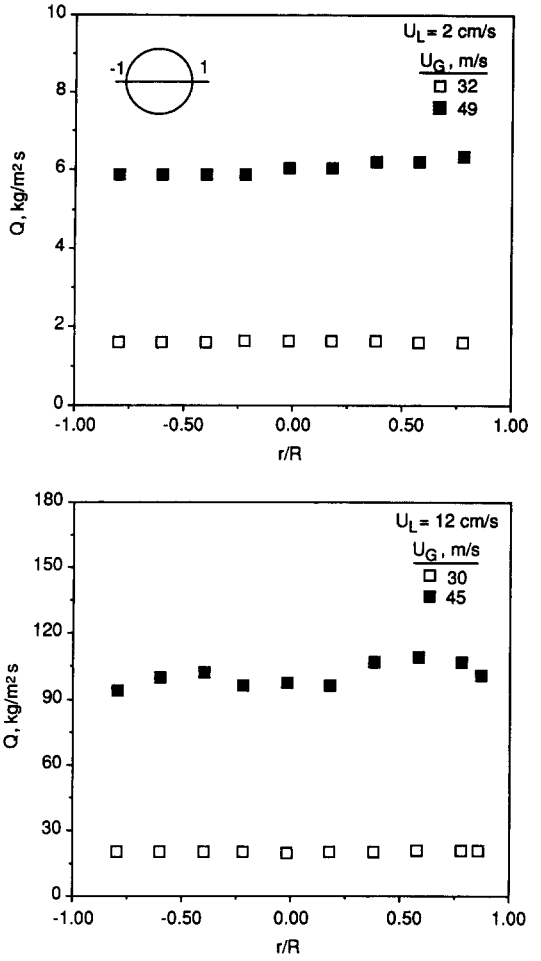

Figure 3. Characteristic horizontal droplet flux profiles.

0.0 and 0.6. It is clear that the mean of three local measurements almost perfectly represents the average flux $\bar{Q}$ in the cross section. Furthermore, the local Q at the centerline is well within 10% of the average.

3. A MODEL FOR PREDICTING DROPLET CONCENTRATION DISTRIBUTION

3.1. The model

Such a model is useful for practical applications; e.g. for developing sampling or measuring procedures of the dispersed phase. It can be also very helpful in the general effort for modeling horizontal annular flow.

Local concentrations seem to be more convenient than fluxes for modeling and data interpretation. The concentration of droplets C (kg/m^3) at a point is calculated by $C = Q/U$, where Q is the local flux (kg/m^{2}s) and U is the local gas velocity (m/s). Local velocities are obtained from the well-known logarithmic expression (Schlichting 1960).

$$\frac{U}{U^*} = 2.5 \ln\left(\frac{y}{K_s}\right) + 8.5, \qquad [1]$$

where U^* is the friction velocity defined as

$$U^* = U_G \sqrt{\frac{f}{2}},$$

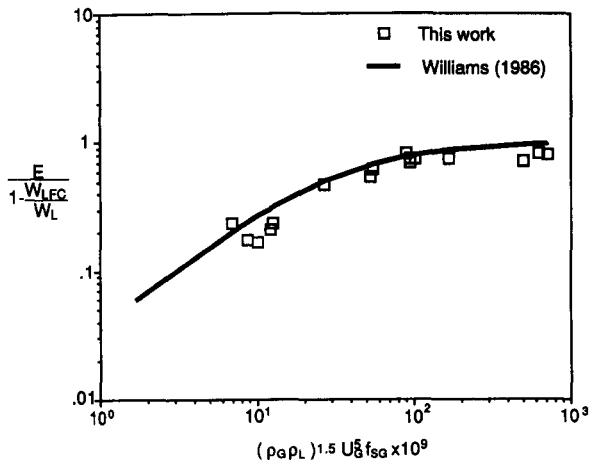

Figure 4. Comparison of entrainment data with the correlation developed by Williams (1986).

f is the friction factor obtained from $\Delta P/\Delta L$ measurements and K_s is the equivalent roughness, given by the following expression:

$$\frac{K_s}{R} = 10^{(0.87 - 0.25 f^{-0.5})} - \frac{9.35}{\mathrm{Re}_G \sqrt{f}},$$

where R is the pipe inside radius and Re_G is the gas phase Reynolds number.

The use of [1] implies that a symmetric velocity profile exists in the pipe. The data by Tsuji & Morikawa (1982) taken under similar conditions, for flow of a dilute particle–gas mixture in horizontal pipes, lend some support to this assumption. Another assumption is that a *uniform* wall roughness exists, due to the wavy liquid film, in the entire pipe circumference regardless of the film asymmetry. RMS values of film thickness measurements (Paras & Karabelas 1991) show that this assumption may be realistic only at relatively high gas velocities, i.e. at $U_G > 40$ m/s.

In the proposed model the following basic assumptions are made:

(i) The entrained liquid in the gas phase is a dispersion of uniform droplet sizes.
(ii) The droplets are small enough so that gas and particle diffusivities are equal, i.e. $\varepsilon_f = \varepsilon$.
(iii) The distribution of droplet fluxes is two-dimensional with respect to the vertical axis. This assumption is supported by the data presented in the previous section.

Using these assumptions a simplified diffusion-type equation is obtained (Karabelas 1977) for the local volume concentration C':

$$\varepsilon \frac{\mathrm{d}C'}{\mathrm{d}y} + wC'(1 - C') = \mathbf{a}'. \qquad [2]$$

The terms on the l.h.s. represent fluxes due to turbulent diffusion and to gravitational settling. In a simplified two-dimensional geometry, and in the absence of other forces, the net flux of droplets ($\mathbf{a}'$) at any horizontal plane is equal to the sum of the above two terms. In general, this sum is not zero. Indeed available experimental evidence (including information presented in section 4 of this paper) suggests that there is a net droplet inflow from the lower part of the pipe surface (where $R_A > R_D$) and a net droplet disappearance at the upper part (where $R_A < R_D$). The parameter $\mathbf{a}'$, therefore, represents a net *upward* flux, which may be considered constant (for a set of flow conditions) in the two-dimensional geometry.

Additional evidence in support of a flux $\mathbf{a}'$ in [2] can be found in the literature. James *et al.* (1980) observed in vertical annular flow that, in the process of liquid atomization, some droplets break off the film surface with large initial velocities. The nearly straight trajectories of such particles may not be significantly influenced either by turbulence or by gravity. Recently, Azzopardi (1987) using

a high-speed photographic technique made similar observations in horizontal annular flow. He reported, among other observations, the following:

> "The drops, which were given a good initial impetus, then travelled upwards until they encountered the wall film. Drops could be seen to feel the effects of gravity and travel in parabolic trajectories. Most drops were seen to travel from the bottom to the top of the tube".

Therefore, such inertia controlled drops (essentially unaffected by turbulence and gravity) give rise to another flux, considered constant at each horizontal plane. This flux can be incorporated in the parameter **a**′ and may play a dominant role in the dynamics of liquid atomization/deposition.

Considering that the droplets in the gas core are in *dilute* dispersion, $C'(1-C) \approx C'$. Indeed, in our tests the mean droplet concentration is <0.003 m^3 water/m^3 air. By multiplying both sides by the liquid density ρ_L, [2] reduces to:

$$\varepsilon \frac{dC}{dy} + wC = \mathbf{a}, \qquad [3]$$

where **a** is the constant flux in kg/m^{2}s, w is the droplet settling velocity (m/s), ε is the eddy diffusivity given by the expression $\varepsilon = \zeta \cdot R \cdot U^*$ and ζ is the dimensionless droplet diffusivity.

By defining

$$\alpha \equiv \frac{\mathbf{a}}{w} \quad \text{and} \quad k \equiv \frac{wR}{\varepsilon} = \frac{w}{\zeta U^*},$$

one obtains

$$\frac{dC}{C-\alpha} = -\frac{k}{R}\,dy. \qquad [4]$$

The solution of [4] leads to

$$C = \alpha + \beta \cdot \exp\left(-k\frac{y}{R}\right), \qquad [5]$$

where β is the constant of integration. This constant (β) can be evaluated by applying the condition that, at steady state, the mean concentration $\hat{C}$ of the droplets along the vertical pipe diameter ($-R \leqslant y \leqslant R$) is known. Thus, the final solution for the distribution becomes

$$\frac{C}{\hat{C}} = A + \frac{1-A}{E(k)}\exp\left(-k\frac{y}{R}\right), \qquad [6]$$

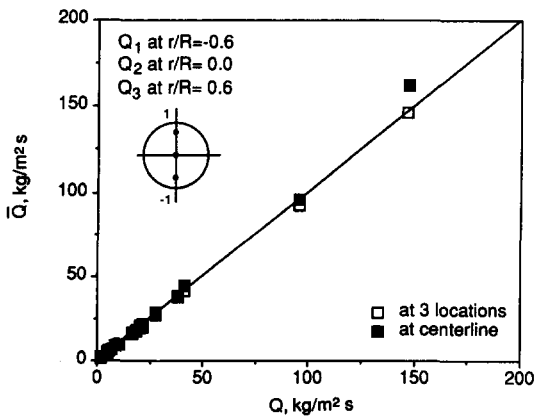

Figure 5. Average flux of liquid entrained in the core against the local flux at the centerline and the arithmetic mean of three local values at $r/D = -0.6$, 0.0 and 0.6.

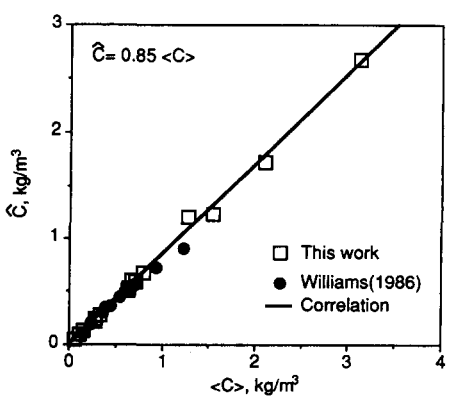

Figure 6. Global average concentration throughout the cross section $\langle C \rangle$ against the average concentration $\hat{C}$ along the vertical diameter.

where

$$A = \frac{\alpha}{\hat{C}} = \frac{\mathbf{a}}{(w\hat{C})}$$

is a dimensionless flux and $E(k) \equiv \sinh(k)/k$. It is evident that only one parameter (the dimensionless flux A) is introduced in the model, in addition to the usual droplet settling velocity and diffusivity. Procedures to compute these quantities are outlined below.

Reliable estimates of a mean droplet diameter are required. Azzopardi (1988) proposed an empirical relation for the Sauter mean diameter, d_{32}, based on available experimental and theoretical studies on drop sizes in vertical annular flow:

$$\frac{d_{32}}{\lambda} = \frac{15.4}{\mathrm{We}^{0.58}} + \frac{3.5\,\bar{Q}}{\rho_L U_G}, \qquad [7]$$

where

$$\lambda = \sqrt{\frac{\sigma}{\rho_L g}}, \quad \mathrm{We} = \frac{\rho_L U_G^2 \lambda}{\sigma}$$

and $\bar{Q}$ is the mean entrained liquid mass flux. A representative mean diameter $d_p = d_{32}/0.7$ (Tatterson *et al.* 1977) will be employed here, with d_{32} obtained from [7]. The computed mean diameters corresponding to our experimental conditions are $<150\,\mu$m, as shown in table 1.

To compute droplet settling velocities, w, a method proposed by Wallis (1974) is used, where

$$w = \frac{U^*}{\left[\dfrac{\rho_G^2}{\mu_G g\,(\rho_L - \rho_G)}\right]^{1/3}},$$

$$u^* = 0.408\,(r^*)^{1.5} \quad \text{for } 1.5 < r^* < 13.4,$$

$$u^* = \frac{1}{3}(r^*)^2 \quad \text{for } r^* < 1.5,$$

and

$$r^* = r_p\left[\frac{\rho_G g(\rho_L - \rho_G)}{\mu_G^2}\right]^{1/3}.$$

Data reviewed by Vames & Hanratty (1988) show that the fluid diffusivity in the core of pipe flow is

$$\frac{\varepsilon_f}{RU^*} = 0.074. \qquad [8]$$

The measurements made by Vames & Hanratty (1988) in a 5 cm pipe as well as the theoretical results obtained by Reeks (1977) and Pismen & Nir (1978) for homogeneous turbulent flow, suggest that for droplet sizes below $100\,\mu$m the ratio of droplet to air diffusivity, $\varepsilon/\varepsilon_f$, is >1. There is, however, considerable uncertainty concerning the true magnitude and the dependence of this quantity upon flow conditions. For the calculations presented here, a dimensionless droplet diffusivity $\zeta = \varepsilon/RU^* = 0.1$ is considered a fair estimate.

The average concentration $\hat{C}$ along the vertical diameter, employed in order to specify a constant of integration [5], is not, in general, equal to the global average $\langle C \rangle$ throughout the cross section. The latter can be readily obtained from the mean flux of entrained liquid $\bar{Q}$ and the mean gas velocity, i.e.

$$\langle C \rangle = \frac{\bar{Q}}{U_G}. \qquad [9]$$

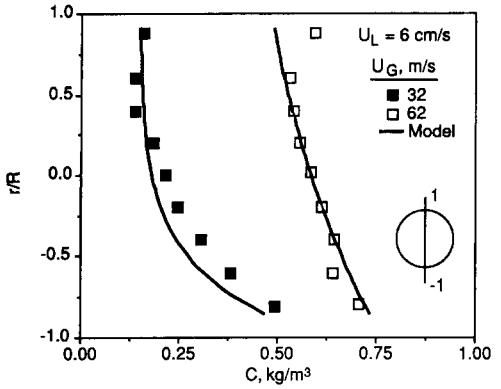

Figure 7. Comparison between data from this investigation along a vertical diameter and model predictions.

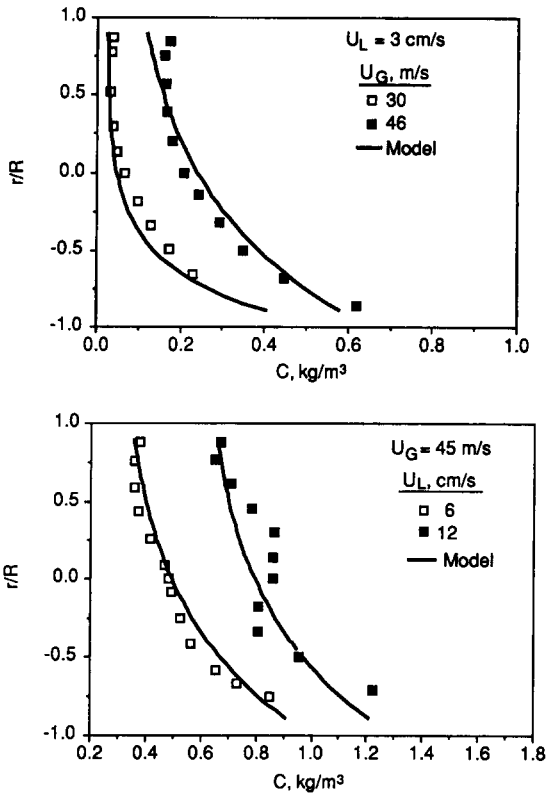

Figure 8. Comparison between data by Williams (1986) along a vertical diameter and model predictions.

To be able to use $\langle C \rangle$, instead of $\hat{C}$, in predictions of concentration distribution, [6], a relationship between the two is required. Figure 6 shows a plot of these quantities extracted from our measurements. It is evident that a simple relationship,

$$\hat{C} = 0.85\langle C \rangle, \qquad [10]$$

represents the data. The same relationship applies to the data by Williams (1986).

3.2. Comparison of data with predictions

Predictions based on this model are in fairly good agreement with the data of this investigation and with the limited data in the open literature (Williams 1986), as shown in figures 7 and 8. The greatest discrepancy between measured and predicted profiles is observed in a few cases at high liquid rates. In those cases, the measured concentration profiles display an inflection point and a local maximum above the pipe centerline. However, before any definite conclusions are drawn, it must be recalled that there is an uncertainty regarding the true velocity distribution, which is required to transform the measured local fluxes to concentrations.

A value of the dimensionless flux A is obtained from the best fit of each profile. It is somewhat surprising that these values cannot be correlated with the gas flow rate. However, the parameter values from our work and from the profiles measured by Williams (1986) show an interesting correlation when plotted against the reduced liquid superficial velocity $U_R = U_L/U_{LC}$ (figure 9). The critical liquid film velocity (U_{LC}) corresponds to the film thickness, attained for high gas flow rates, below which there is no atomization. Values of the critical film flow rate W_{LFC}, from which U_{LC} is computed, for $D = 50$ and 100 mm, are given by Laurinat (1982) and Williams (1986). Figure 9 suggests that there is a correlation between A and U_L/U_{LC}. The line in figure 9 has been drawn so that the flux $A \to 0$ as the liquid velocity approaches its critical value, i.e. as $(U_L/U_{LC}) \to 1.0$ at which no atomization can occur.

Figure 10 shows values of A from this study plotted vs dimensionless average atomization rates $\overline{R_A^+}$ presented in the next section. It is tacitly assumed here that under steady-state conditions

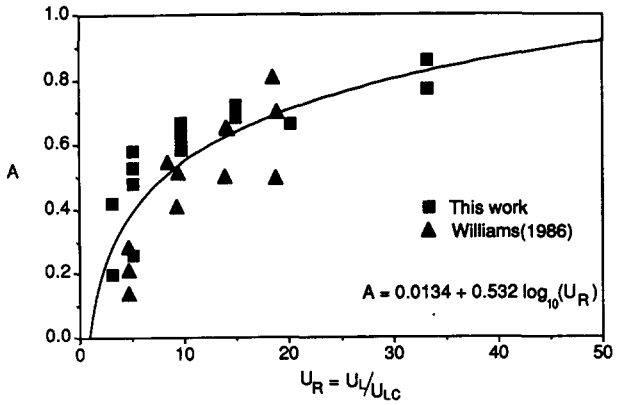

Figure 9. Influence of reduced liquid velocity on model parameter A.

$\overline{R_D^+} = \overline{R_A^+}$. The very good correlation between these quantities lends support to the interpretation offered for A. Indeed, an obvious physical significance can be attached to the fact that the dimensionless flux A tends to increase rather sharply with mean atomization rate $\overline{R_A^+}$, at low $\overline{R_A^+}$, and to reach a constant value at high $\overline{R_A^+}$.

4. DROPLET DEPOSITION RATES

4.1. Local deposition rates

Deposition rates of droplets (R_D) are calculated from our experimental data by assuming that deposition is a diffusion-like process, so that

$$R_D = k_D \cdot C, \qquad [11]$$

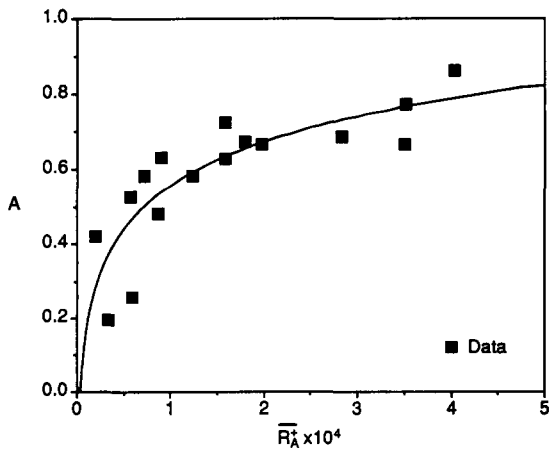

Figure 10. Variation of the parameter A with the dimensionless average atomization rate $\overline{R_A^+}$.

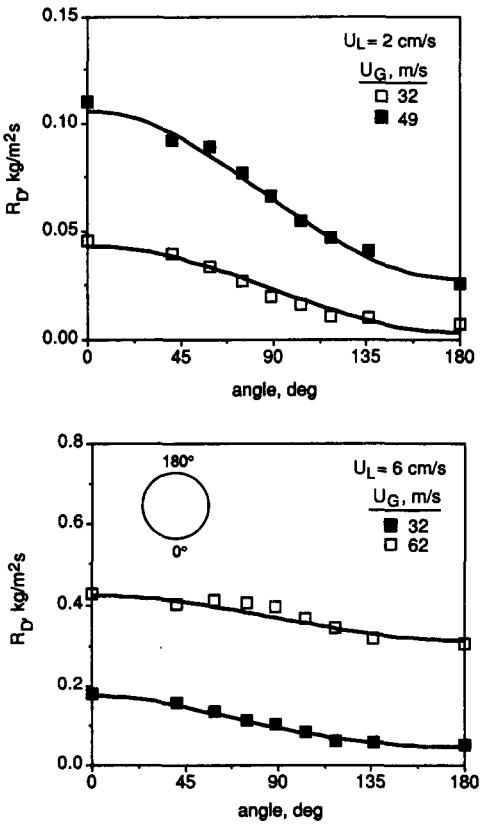

Figure 11. Circumferential distribution of the deposition rate.

where k_D is the deposition rate constant (m/s) and C (kg/m^3) is the local droplet concentration close to the pipe wall. The droplet concentration on the film surface is assumed to be zero.

The local concentration at a distance 5 mm from the wall (available from direct measurements or extrapolation) is considered quite representative of C. This distance is the nearest to the solid wall where local flux measurements are made, and is always greater than the maximum wave height at the pipe bottom. Obviously, the values of C thus obtained are the best estimates we can presently make on the circumferential variation of the droplet concentration close to the wall. An attempt to measure or estimate C at a distance closer to the wall is not expected to provide more accurate results due to possible errors introduced either by the wavy interface, or by the (essentially unknown) local velocity distribution required to transform local fluxes to local concentrations.

Correlations of k_D/U^*, reviewed by McCoy & Hanratty (1977), are used to calculate the deposition rate k_D. For the droplet sizes corresponding to our measurements, the expression

$$k_D = 20.7 \cdot U^* \cdot (\tau^+)^{-0.5}, \quad [12]$$

which is valid for $\tau^+ > 3000$, is employed. The dimensionless relaxation time τ^+ is defined as

$$\tau^+ = \frac{d_p^2 (U^*)^2 \rho_G \rho_p}{18 \mu_G^2}, \quad [13]$$

where U^* is the friction velocity and the subscripts p and G designate particle and gas properties, respectively.

Local deposition rates along the pipe circumference are obtained from our data. Figure 11 shows typical R_D circumferential distributions for various gas and liquid rates. Most of the profiles exhibit a smooth variation with the maximum R_D at the pipe bottom. The data by Anderson & Russell (1970) display the same trend. However, some distributions display an uneven variation (with other local maxima), caused by the peculiarities of the corresponding experimental flux distributions. High gas velocities promote nearly uniform R_D distribution. The data were fitted with a three-parameter exponential expression [recommended by Laurinat (1982)] to facilitate integration and computation of average R_D. The lines in figure 11 were obtained from such a fit. An attempt to correlate the average deposition rates follows.

4.2. Interpretation of deposition rates

It is generally accepted that under steady-state conditions, prevailing in our experiments, the average deposition rate, $\overline{R_D}$, is equal to the average atomization rate, $\overline{R_A}$, in the pipe circumference. We shall, therefore, attempt to correlate the average $\overline{R_D}$ data by using theoretical arguments advanced in order to interpret atomization rates $\overline{R_A}$.

Woodmansee & Hanratty (1969), following the work of Taylor (1940), propose that droplet atomization is essentially due to a Kelvin–Helmholtz instability-type mechanism, whereby pressure variations, in the air flowing over wavelets, overcome the stabilizing forces of gravity and surface tension. Furthermore, they recommend a Weber number criterion (We = 5.5) for incipient atomization, where We is defined as

$$\mathrm{We} = \frac{\rho_G U_{rel}^2 h_w}{\sigma}. \quad [14]$$

The height of disturbance waves h_w is used as the characteristic length and $U_{rel} = U_G - U_c$, the gas velocity relative to disturbance wave celerity.

It is of great interest to apply the above criterion to horizontal flow which is characterized by circumferentially varying films. In order to compute the variable large-wave height h_w and the respective wave celerity U_c, data reported in the companion paper (Paras & Karabelas 1991) are employed. The simple expression

$$h_w = 4(\mathrm{RMS}) \quad [15]$$

is used to calculate the circumferential variation of h_w at any point on the tube periphery from already available distributions of the RMS of the film thickness. This equation correlates very satisfactorily our experimental data at locations $\Theta = 0°$, 45° and 90°. The most complete data set is the one at $\Theta = 0°$ (pipe bottom).

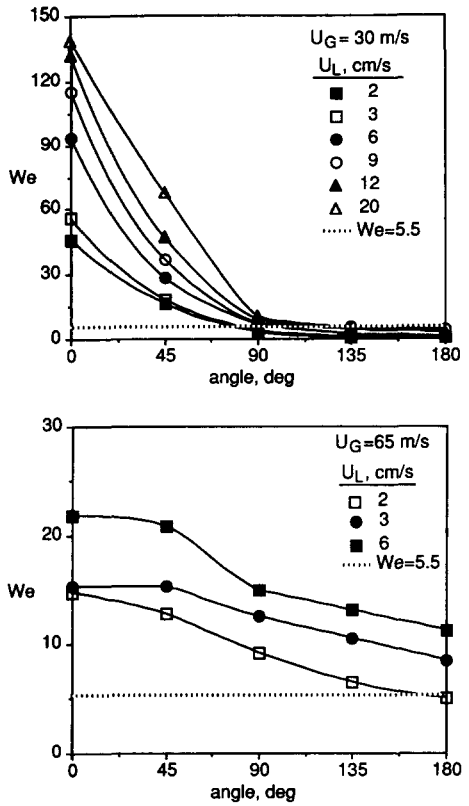

Figure 12. We distribution around the circumference for relatively small and large gas velocities

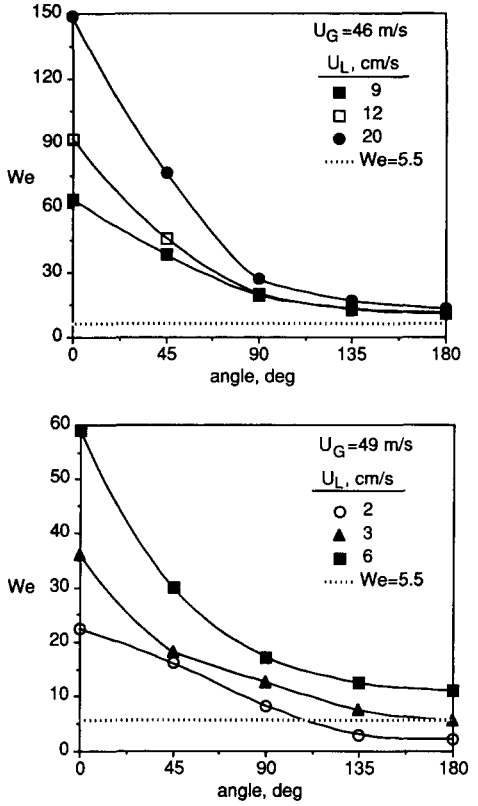

Figure 13. We distribution around the circumference for intermediate gas velocities.

Figures 12 and 13 show the circumferential We distributions under various conditions. The criterion We = 5.5 suggests that at relatively *small gas velocities* (e.g. $U_G = 30$ m/s, figure 12) atomization cannot take place from the film in the upper half of the pipe, over the entire range of liquid flow rates investigated. However, at relatively *large gas velocities* (e.g. $U_G = 65$ m/s, figure 12) atomization can occur from the entire pipe circumference. At intermediate gas flow rates (figure 13), it appears that the main contribution to entrainment comes from the lower half of the pipe, with a relatively minor contribution from the rest of the film.

The above results are in agreement with other experimental evidence (Paras & Karabelas 1991), showing that large disturbance waves (moving in the lower part of the pipe at small U_G) tend to cover gradually larger portions of the circumference with increasing gas velocity. Furthermore, the above evidence indicates that atomization very likely occurs only from the top of large disturbance waves. The loss of liquid due to entrainment and the associated surface deformation may also offer an explanation as to why the shape of large disturbance waves tends to change quite rapidly (Paras & Karabelas 1991).

In a recent study on *vertical* annular flow, Schadel & Hanratty (1989) recognize the significance of large disturbance waves on atomization and suggest that (in low viscosity liquids) We may lead to a satisfactory correlation of dimensionless atomization (or deposition) rates, defined as

$$R_A^+ = \frac{R_A}{U_G\sqrt{\rho_G \rho_L}}. \qquad [16]$$

They recommend a We defined as in [14] or in terms of a friction velocity. To better take into account the effect of disturbance waves, Schadel & Hanratty (1989) recommend a correlation of the type

$$R_A^+ = \mathbf{I} \cdot f(\mathrm{We}), \qquad [17]$$

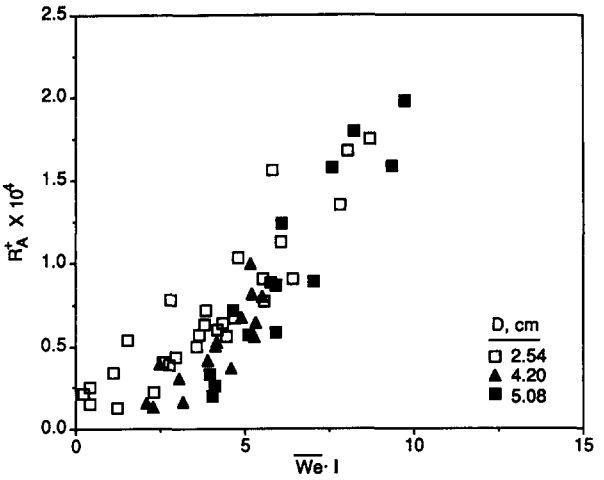

Figure 14. Relationship between the dimensionless deposition rate R_A^+ and $\overline{We} \cdot \mathbf{I}$.

where **I** is the large-wave intermittency, i.e. the fraction of time disturbance waves are present on the film.

In view of the successful application of We criteria (in order to determine the regions of the film contributing to atomization), we explore the use of [17] to correlate *average* atomization (or deposition) rates in horizontal annular flow as well. Figure 14 shows dimensionless rates (R_A^+) measured by Schadel & Hanratty (1989), plotted together with rates ($\overline{R_D^+}$) obtained in this work ($D = 5.08$ cm). Average Weber numbers ($\overline{We}$) are computed from the We distributions, such as those depicted in figures 12 and 13. The intermittencies **I** are extracted from the film thickness records at $\Theta = 0°$ (Paras & Karabelas 1991), for each pair of gas and liquid rates. It will be recalled that in this work **I** is found to be quite insensitive to U_G and U_L changes, and to vary within a narrow range of values around 0.40.

Figure 14 suggests that, for low viscosity liquids, a linear relationship may exist between R_A^+ and $\mathbf{I} \cdot \overline{We}$. The fairly good correlation of the data is surprising, considering the uncertainties involved in estimating **I**, the entirely different approaches employed to obtain R_D and the different main flow directions of the two studies. In addition to liquid properties (mainly viscosity and surface tension), which are constant in the tests, the influence of pipe diameter cannot be assessed at present. Indeed, the scatter in the data and the small range of diameters employed do not permit that.

One of the difficulties experienced, in trying to use a correlation of the type $R_D^+ = f(\overline{We} \cdot \mathbf{I})$, is the estimation of $\overline{We}$ as a function of flow conditions. One approach may be to start with an estimate (from experiments or otherwise) of h_w or film height RMS at the bottom (RMS_0). Then one could use the expression

$$\frac{RMS_0}{\langle RMS \rangle} = 8.43 - 0.107\, U_G, \qquad [18]$$

which correlates average $\langle RMS \rangle$ in the pipe with gas velocity and the expression $h_w = 4.0$ (RMS) at any angular position to compute We as a function of U_G. The intermittency **I** could be taken as roughly constant (≈ 0.40).

It is pointed out here that the values of R_D obtained in this study are not correlated when plotted vs an excess liquid rate $(W_{LF} - W_{LFC})/\pi D$. On the contrary, Schadel & Hanratty (1989) report an excellent correlation of their R_A data with excess liquid rate.

5. CONCLUDING REMARKS

Analyses of local droplet flux measurements and of local film thickness time records provide a considerable amount of new information on liquid entrainment and deposition in horizontal annular flow. Local flux profiles display a nearly two-dimensional distribution, i.e. almost constant values along horizontal chords of the pipe cross section. Integrating such profiles provides reliable

data on the mean liquid entrainment fraction E, which are in good agreement with a correlation proposed by Williams (1986).

The circumferential distribution of deposition rate R_D is obtained by assuming that the common linear rate expression $R_D = k_D \cdot C$ holds with an estimated local concentration close to the wall. The results appear to be quite consistent and in qualitative agreement with the data of Anderson & Russell (1970). However, additional measurements, with a differential technique, are required to examine the accuracy of these results and to test the validity of the linear rate expression.

A We criterion (We = 5.5) has been proposed by Woodmansee & Hanratty (1969) to represent incipient atomization in horizontal air–water channel flow. The wave height h_w has been used as the characteristic length in We. Using our data (Paras & Karabelas 1991) on the circumferential variation or large-wave height and the criterion We = 5.5, it has been shown that only at relatively high gas velocities can atomization take place in the upper half of the pipe.

The average deposition rates $\overline{R_D^+}$ from this work, plotted vs $(\overline{We} \cdot \mathbf{I})$, are in surprisingly good agreement with average R_A^+ measurements by Schadel & Hanratty (1989) obtained in vertical flow. The nearly linear dependence of average rates ($\overline{R_A^+}$ or $\overline{R_D^+}$) on $(\overline{We} \cdot \mathbf{I})$, for both horizontal and vertical flow, may point in the direction of a generalized correlation.

A simple phenomenological model is proposed for predicting the droplet concentration distribution in the gas phase. A dimensionless parameter A is considered to represent a combination of fluxes; i.e. the flux of drops which gain high inertia upon liquid film atomization and tend to travel straight to the opposite pipe wall, and the net upward flux of small droplets which are affected by turbulence. The observation that, at relatively low and moderate gas velocities, only the film in the *lower* part of the pipe contributes to atomization lends support to the use of this parameter. Figure 10, showing a strong dependence of A on the average atomization rate R_A^+, provides additional support.

An attempt to correlate A with a reduced liquid superficial velocity, U_L/U_{LC}, is presented in figure 9. Estimates of the critical velocity U_{LC} are available for pipe dia 2.5–10 cm (Williams 1986). One can therefore, predict droplet concentration or flux distributions, given the pipe i.d. and gas and liquid flow rates, as follows. From an entrainment correlation (e.g. Williams 1986) the global concentration $\langle C \rangle$ is obtained and the concentration (or flux) distribution along the vertical diameter is then computed from [6] and [10]. Assuming a two-dimensional flux distribution and an axisymmetric velocity profile, local concentrations can be calculated at any point in the core of the cross section. One can further compute the circumferential R_D distribution as well as the average $\overline{R_D^+}$. Although quite convenient for practical calculations and modeling, this model is fairly rough and relies on several physical quantities which have not been firmly established yet. Such quantities are the droplet size distribution, droplet and gas velocity distributions in the cross section, droplet diffusivity—to mention only a few. Work to determine some of these quantities is in progress.

Acknowledgements—Financial support by the Commission of European Communities (Contract No. EN3G-0040-GR) and the General Secretariat for Research & Technology of Greece is gratefully acknowledged.

The authors also wish to thank Drs N. Andritsos and V. Bontozoglou for their helpful comments and suggestions.

REFERENCES

ANDERSON, R. J. & RUSSELL, T. W. F. 1970 Film formation in two-phase annular flow. *AIChE Jl* **14,** 626–633.

AZZOPARDI, B. J. 1987 Observations of drop motion in horizontal annular flow. *Chem. Engng Sci.* **42,** 2059–2062.

AZZOPARDI, B. J. 1988 The role of drops in annular gas–liquid flow: drop sizes and velocities. *Jap. J. Multiphase Flow* **2,** 15–35.

FUKANO, T. & OUSAKA, A. 1989 Prediction of the circumferential distribution of film thickness in horizontal and near-horizontal gas–liquid annular flows. *Int. J. Multiphase Flow* **15,** 403–420.

HUTCHINSON, P. & WHALLEY, P. B. 1973 A possible characterization of entrainment in annular flow. *Chem. Engng Sci.* **28,** 974–975.

JAMES, P. W., HEWITT, G. F. & WHALLEY, P. B. 1980 Droplet motion in two-phase flow. UKAEA Report AERE-R 97 11.

KARABELAS, A. J. 1977 Vertical distribution of dilute suspensions in turbulent pipe flow. *AIChE Jl* **23,** 426–434.

LAURINAT, J. E. 1982 Studies of the effects of pipe size on horizontal annular two-phase flows. Ph.D. Thesis, Univ. of Illinois, Urbana.

LAURINAT, J. E., HANRATTY, T. J. & JEPSON, W. P. 1985 Film thickness distribution for gas–liquid annular flow in a horizontal pipe. *PhysicoChem. Hydrodynam.* **6,** 179–195.

LEMAN, G. W. 1975 Atomization and deposition in two phase annular flow: measurement and modelling. Ph.D. Thesis, Univ. of Illinois, Urbana.

LIN, T. F., JONES, O. C., LAHEY, R. G., BLOCK, R. C. & MURASE, M. 1985 Film thickness measurements and modelling in horizontal annular flows. *PhysicoChem. Hydrodynam.* **6,** 197–206.

MCCOY, D. D. & HANRATTY, T. J. 1977 Rate of deposition of droplets in annular two phase flow. *Int. J. Multiphase Flow* **3,** 319–331.

PARAS, S. V. & KARABELAS, A. J. 1991 Properties of the liquid layer in horizontal annular flow. *Int. J. Multiphase Flow* **17,** 439–454.

PISMEN, L. M. & NIR, A. 1978 On the motion of suspended particles in stationary homogeneous turbulence. *J. Fluid Mech.* **84,** 194.

REEKS, M. W. 1977 On the dispersion of small particles suspended in an isotropic turbulent fluid. *J. Fluid Mech.* **83,** 529.

ROMANO, G., DELLA LATTA, G. & ANDREUSSI, P. 1978 The measurement of entrained liquid flowrate in annular downward flows. *Ing. Chim. Ital.* **14,** 84–89.

SCHADEL, S. A. 1988 Atomization and deposition rates in vertical annular two-phase flow. Ph.D. Thesis, Univ. of Illinois, Urbana.

SCHADEL, S. A. & HANRATTY, T. J. 1989 Interpretation of atomization rates of the liquid film in gas/liquid annular flow. *Int. J. Multiphase Flow* **15,** 893–900.

SCHLICHTING, H. 1960 *Boundary Layer Theory*, 4th edn. McGraw-Hill, New York.

TATTERSON, D. F., DALLMAN, J. C. & HANRATTY, T. J. 1977 Drop sizes in annular gas–liquid flows. *AIChE Jl* **23,** 68–76.

TAYLOR, G. I. 1940 Generation of ripples by wind blowing over a viscous fluid. Reprinted in *The Scientific Papers of Sir Geoffrey Ingram Taylor*, Vol. 3, pp. 244–255. Cambridge Univ. Press, London (1963).

TSUJI, Y. & MORIKAWA, Y. 1982 LDV measurements of an air–solid two-phase flow in a horizontal pipe. *J. Fluid Mech.* **120,** 385–409.

VAMES, S. & HANRATTY, T. J. 1988 Turbulent dispersion of droplets for air flow in a pipe. *Expts Fluids* **6,** 94–104.

WALLIS, G. B. 1975 The terminal speed of simple drops or bubbles in an infinite medium. *Int. J. Multiphase Flow* **1,** 491–511.

WILLIAMS, L. R. 1986 Entrainment measurements in a 4 inch horizontal pipe. M.Sc. Thesis, The Univ. of Illinois, Urbana.

WOODMANSEE, D. F. & HANRATTY, T. J. 1969 Mechanism for the removal of droplets from a liquid surface by a parallel air flow. *Chem. Engng Sci.* **24,** 299–307.